doi: 10.18720/MCE.76.24

Methods of identification of concrete elastic-plastic-damage models

Методы идентификации упруго-пластических моделей бетона с учетом накопления повреждений

A.V. Benin,
Petersburg State Transport University, St. Petersburg, Russia
A.S. Semenov,
S.G. Semenov,
M.O. Beliaev,
V.S. Modestov,
Peter the Great St. Petersburg Polytechnic University, St. Petersburg, Russia

Канд. техн. наук, заведующий ИЛ "Механическая лаборатория им. проф. Н.А. Белелюбского" А.В. Бенин,
Петербургский государственный университет путей сообщения Императора Александра I, г. Санкт-Петербург, Россия
канд. физ.-мат. наук, доцент А.С. Семенов,
инженер С.Г. Семенов,
студент М.О. Беляев,
ведущий инженер В.С. Модестов,
Санкт-Петербургский политехнический университет Петра Великого, г. Санкт-Петербург, Россия

Key words: concrete; parameter identification; elasticity; plasticity; damage; experiment; finite-element simulation

Ключевые слова: бетон; идентификация параметров материала; упругость; пластичность; повреждение; эксперимент; конечно-элементное моделирование

Abstract. The methodology for identification of mechanical characteristics of the nonlinear material model for concrete, taking into account the elastic-plastic deformation and the damage accumulation under monotonous and cyclic loading, is proposed. The using such improved models of concrete deformation is actual for carrying out finite-element computations of the most important elements of unique and responsible buildings and structures. The proposed methodology is verified for three different types of concrete (B45, B25, B5), including also their preliminary heat treatment at 200 °C, 300 °C, 400 °C and 600 °C. The experiments were carried out on standard specimens of cubic and prismatic form under compression, as well as on dog-bone-shaped specimens under tension. Elasticity and plasticity moduli, ultimate strengths in compression and tension, damage evolutions during deformation process were obtained in tests. Particular attention has been paid to the search for reliable and effective methods for determining damage based on cyclic deformation curves in the pre-peak and after-peak loading regimes. Comparison of simulation results with experimental data under monotonic and cyclic compression demonstrates a good agreement for regular and for overheated concrete.

Аннотация. Предложена методика идентификации механических характеристик модели неупругого деформирования бетона, учитывающая упруго-пластическое деформирование и накопление повреждений при монотонном и циклическом нагружении. Использование подобных уточненных моделей деформирования бетона актуально при проведении конечно-элементных расчетов наиболее ответственных узлов уникальных зданий и сооружений. Методика верифицирована для трех различных сортов бетона (B45, B25, B5), включающих также их предварительную термическую обработку при 200 °C, 300 °C, 400 °C и 600 °C. Эксперименты выполнялись на стандартных кубических и призматических образцах при сжатии, а также на образцах-восьмерках при растяжении. В процессе идентификации определялись упругие и пластические модули, характеристики прочности при сжатии и растяжении, а также зависимости характеризующие процесс накопления повреждений с ростом пластических деформаций. Особое внимание уделялось поиску надежных и эффективных методов определения поврежденности на основе кривых циклического деформирования в допиковой и запиковой областях нагружения. Сравнение полученных результатов конечно-элементных расчетов с использованием предложенной модели материала с экспериментальными данными продемонстрировало хорошее соответствие для стандартных и термообработанных бетонов.

Бенин А.В., Семенов А.С., Семенов С.Г., Беляев М.О., Модестов В.С. Методы идентификации упруго-пластических моделей бетона с учетом накопления повреждений // Инженерно-строительный журнал. 2017. № 8(76). С. 279–297.

Introduction

The elastic-plastic models with account of damage accumulation [1–6] provide effective tools for the modeling nonlinear concrete behavior [7, 8] with taking into account irreversible deformation after unloading, softening effect after strength peak, inelastic volumetric expansion and stiffness degradation. The considered class of concrete models is able also to describe different damage nature under tension (due to progressive microcracking) and under compression (because of crushing); permanent degradation of material stiffness under cyclic loading conditions; stiffness recovery while transiting from tension to compression; anisotropy of mechanical characteristics (concerning strength, hardening, damage) under tension and compression.

There are many numerical implementations of such type of material models, for example, in commercial software ABAQUS [9]. One of the main difficulties in use of such models in practice is an identification of the material parameters for the computation of real concrete and reinforced concrete structures [10–13]. There are few resent researches aimed to obtain all parameters for elastic-plastic-damage model [14, 15]. A calibration of concrete parameters based on digital image correlation was proposed in [16]. Analytical methods of concrete stress-strain analysis under cyclic loading with taking into account of creep are used in [17, 18]. Features of the concrete behavior at elevated temperatures are considered in [15, 19].

The main aim of the study is development of the methodology for the elastic-plastic-damage concrete model parameter identification. To achieve the goal, the following tasks were accomplished:

- design of test setup for the correct control test and obtaining stress-strain curves;
- carrying out experiments using recommended Russian State Standard specimens [20] and identifying model parameter;
- search for reliable and effective methods for damage evaluation based on cyclic deformation curves in the pre-peak and after-peak loading regimes;
- validation of identified parameters using finite-element computations of stress-strain state and fracture of experimental specimens and structural elements.

To use the concrete damage plasticity model in ABAQUS [9] the following concrete parameters must be experimentally defined and set:

- initial (undamaged) elastic moduli (E_0, v_0);
- plasticity characteristics (stress-strain curves under compression σ_c (ε_{in}) and under tension σ_t (ε_{cr}), dilation angle β; flow potential eccentricity m;. the ratio of initial equibiaxial compressive yield stress to initial uniaxial compressive yield stress f_{b0} / f_c; the ratio K_c of the second stress invariant on the tensile meridian to that on the compressive meridian);
- viscosity parameter μ, used for the visco-plastic regularization of the concrete constitutive equations;
- damage evolution diagrams under compression D_c (ε_{in}) and under tension D_t (ε_{cr}).

The procedure of plasticity parameters identification is considered in detail in [14].

To determine material parameters the following types of experiments are necessary in general case:

- monotonic uniaxial compression test;
- monotonic uniaxial tension test;
- biaxial loading test;
- cyclic loading test.

The main focus of this paper is on the definition of the concrete damage based on cyclic stress-strain curves. The curves of monotonous loading are not sufficient to determine the plastic deformation and damage of concrete therefore an analysis of the cyclic deformation curves is necessary for our aims. The results of previous basic experimental investigations of concrete under cyclic loading are presented in [21–25] for compression and in [26–28] for tension. In dimensionless coordinates the cyclic stress-strain curves under tension (Fig. 1b) demonstrate a larger scattering than the curves under compression (Fig. 1a). However, in both cases, nonlinearities of the unloading and reloading branches are observed for each cycle. This presents the main difficulty in identifying the damage. To eliminate this uncertainty a comparison of 30 different (known and original) methods for determining the degraded stiffness is performed in this paper with taking into account the conditions of admissible values of the damage, the monotonic damage growth, and the localization conditions. The validation of the considered methods is

Benin A.V., Semenov A.S., Semenov S.G., Beliaev M.O., Modestov V.S. Methods of identification of concrete elastic-plastic-damage models. *Magazine of Civil Engineering*. 2017. No. 8. Pp. 279–297. doi: 10.18720/MCE.76.24.

carried out on the basis of comparison with the results of the performed tests and verification in the finite element simulations of characteristic structural elements.

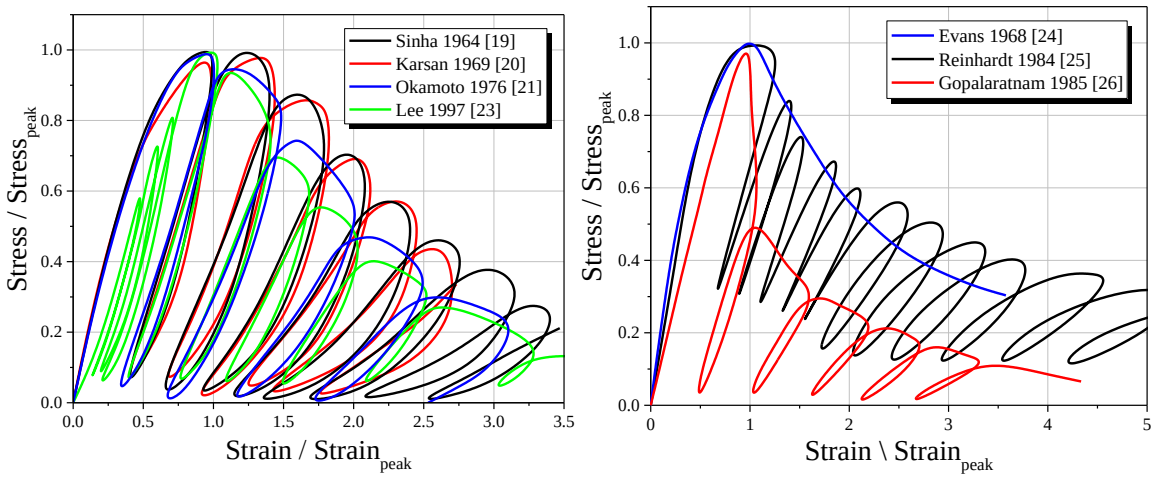

a) **b)**

Figure 1. Cyclic stress-strain curves: a) compression and b) tension for various concretes [21–28]

Methods

Test setup

The test setup (Fig. 2a) is based on Shimadzu AGX300 electromechanical test machine. The fixtures (Fig. 2b) for tensile tests and deformation sensor frame (Fig. 2c) were designed and produced.

a) **b)** **c)**

Figure 2. Test machine (a), tensile test fixtures (b) and strain sensor frame (c)

There are two Heidenhain ST1278 length gauge sensors used for strain measurement. The sensors were interfaced with test machine controller and result strain was calculated as average of two sensors measurements for neglecting influence of bending effect. The strain sensor frame was installed directly on the specimen. This approach allows obtaining the direct strain measurement during testing and as result to measure correctly elastic modulus (see, for example, comparison of modules measured by different methods in table 2 from [15]). Such design allows to perform experiments in the temperature chamber and using quartz glass tubes for precisely strain measurement.

Specimens

Specimens were prepared according to the recommendation of Russian State Standard [22]. There are three types of specimens:

- cubes 100×100×100 mm for concrete class (cube strength) definition,
- prisms 100×100×400 mm for compression experiments,
- dog-bone specimens for tension experiments.

The samples were made from three different types of concrete with standard cube strength class of:

- B45 (Concrete 1),
- B25 (Concrete 2),
- B5 (Concrete 3).

Concrete mixture recipe for Concrete 1 is 400 kg/m^3 of CEM I 42.5R, 700 kg/m^3 of 0/4 gabbro sand, 1125 kg/m^3 of 5/10 gabbro coarse aggregate, 120 kg/m3 of fly-ash, 230 kg/m^3 of water and 35 kg/m^3 of plasticizers and modifiers; for Concrete 2 is 410 kg/m^3 of CEM I 42.5R, 340 kg/m^3 of 0/5 haydite sand, 400 kg/m^3 of 5/10 claydite gravel, 95 kg/m3 of fly-ash, 216 kg/m^3 of water and 40 kg/m^3 of modifiers; for Concrete 3 is 180 kg/m^3 of CEM I 42.5R, 185 kg/m^3 of 0/5 haydite sand, 150 kg/m^3 of 5/10 claydite gravel, 120 kg/m3 of fly-ash, 130 kg/m^3 of water and 25 kg/m^3 of plasticizers and modifiers. Specimens were casted in standard steel forms, extracted from forms after 3 days and cured in the 95% humidity and 20°C temperature environment during 28 days.

A part of specimens have a preliminary heating treatment at temperatures at 200 °C, 300 °C, 400 °C and 600 °C. The heating rate was 10 °C/h. It should be noted that when overheating concrete at temperature higher than 400 °C a network of cracks appears (Fig. 3). While overheating at temperature of up to 600 °C with increased heating rate of 100 °C/h, which simulated the emergency mode, a specimen of Concrete 2 exploded in the furnace.

Some microstructural stresses appear in the process of heating, being caused by different coefficients of linear expansion of aggregate and matrix or by other processes, which requires a special individual study.

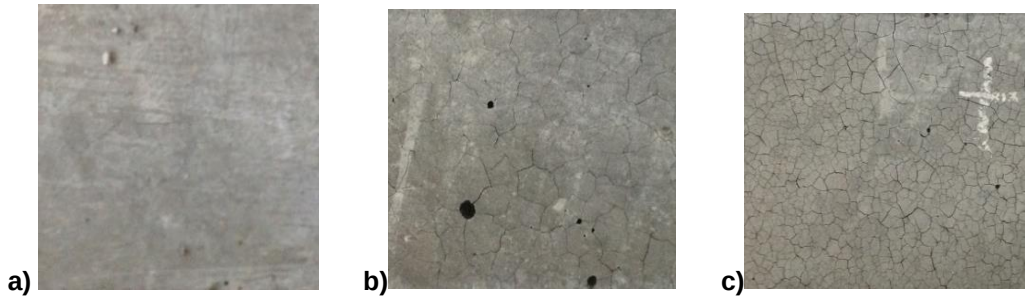

Figure 3. Surfaces of Concrete 2 specimens with different overheating temperatures: a) 300°C, b) 400°C, c) 600°C

Results and Discussion

Experimental results

As a result of numerous experiments, the following data were obtained:

- cube strength for Concrete 1,2,3 at 20°C;
- concrete-to-steel bond strength at different test temperatures (Concrete 1);
- monotonic compression stress-strain curves for Concrete 1,2,3 for different overheating temperatures;
- monotonic tension stress-strain curves for Concrete 1,2,3 for different overheating temperatures;
- cyclic compression stress-strain curves for Concrete 1,2,3 for different overheating temperatures;
- cyclic tension stress-strain curves for Concrete 1,2,3 for different overheating temperatures.

Typical cyclic stress-strain curves containing the post-peak behavior under compression and tension for the specimens from the overheated concrete are given in Figs. 4a and b. These curves are basis for the parameter determination of the evolution law for the plastic strain and damage.

Specimens from non-overheated concrete show in experiments a sudden failure, displacement instability and snap-back phenomena usually in the softening branch. It is especially difficult to obtain the tensile curves (see Fig. 4b). Therefore pure load or displacement control test techniques are not enough to control the whole test including softening branch. The optimal test technique is a mixed control system [29, 30]. Specimens from the overheated concrete allow for more easily to measure the after-peak behavior (compare Figs. 4c,d with Figs. 4a,b). Carrying out experiments on such concretes opens the possibility of investigating in more detail the post-peak behavior on test machines with standard control.

Failure modes of specimens under compression and tension are shown in Figure 5 for Concrete 1,2,3. Overheating and concrete type have no significant effect of failure mode. The greatest differences are observed when comparing tension and compression.

The overheating has a significant effect on the elastic modulus and strength (Fig. 6). A noticeable drop in properties is observed after 300 °C. This correlates well with the appearance of cracks network (Fig. 3).

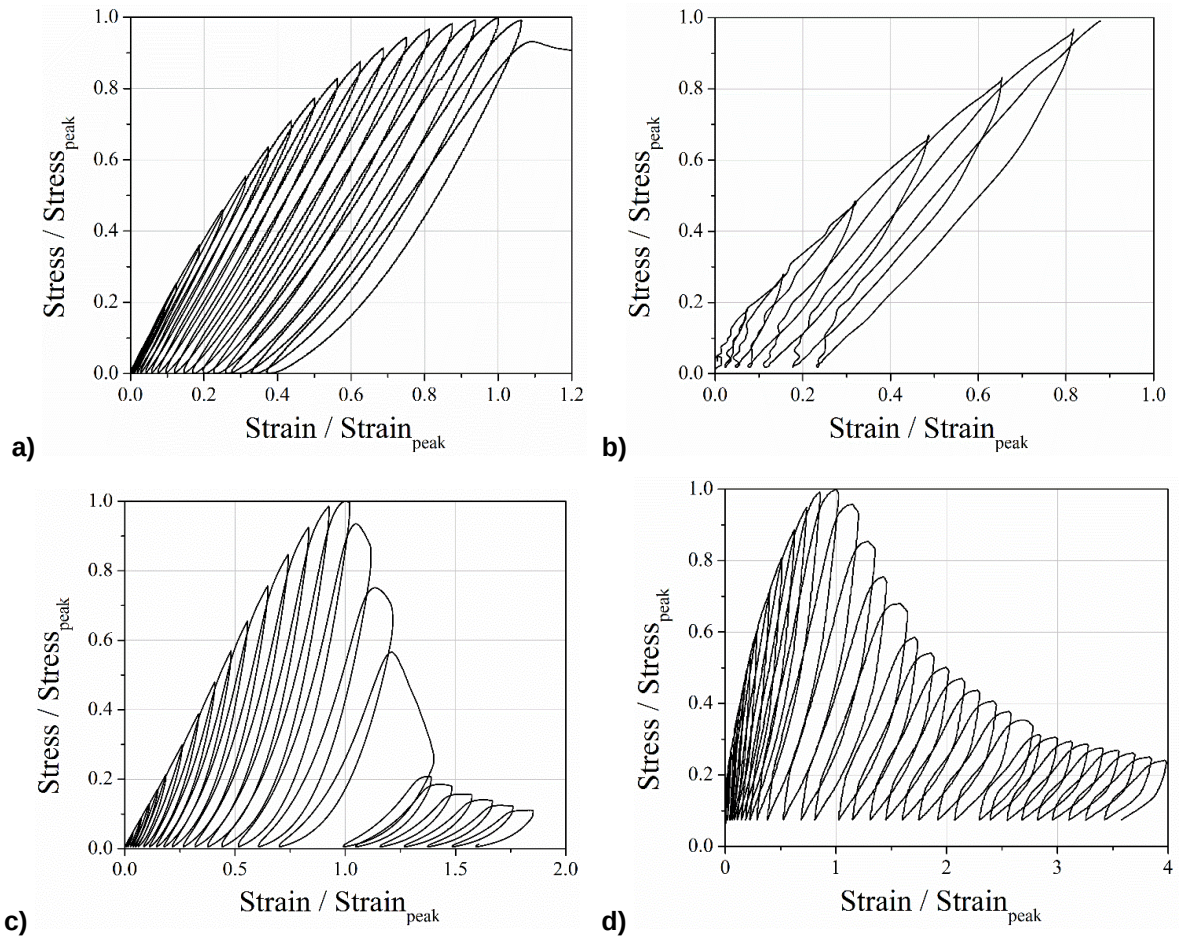

Fig. 4. Typical cyclic stress-strain curves for Concrete 1:
a) compression (non-overheated), b) tension (non-overheated),
c) compression (overheated at 600°C), d) tension (overheated at 600°C)

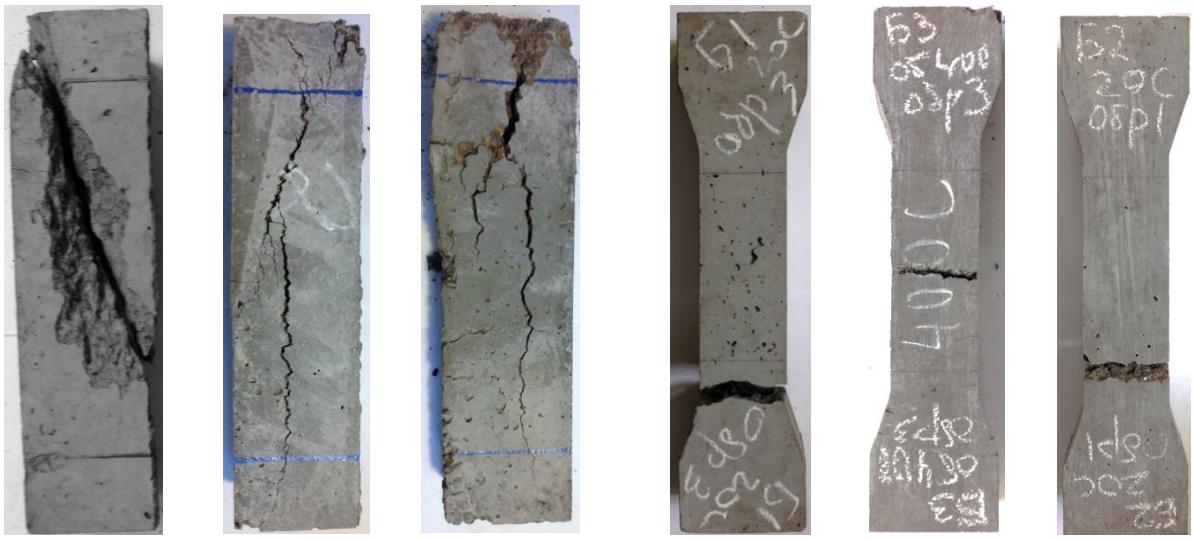

a) b) c) d) e) f)

Figure 5 Failure modes: a) compression of non-overheated Concrete 1, b) compression overheated at 400°C Concrete 2, c) compression of non-overheated Concrete 3, d) tension of non-overheated Concrete 1, e) tension of overheated at 400°C Concrete 2, f) tension of non-overheated Concrete 3

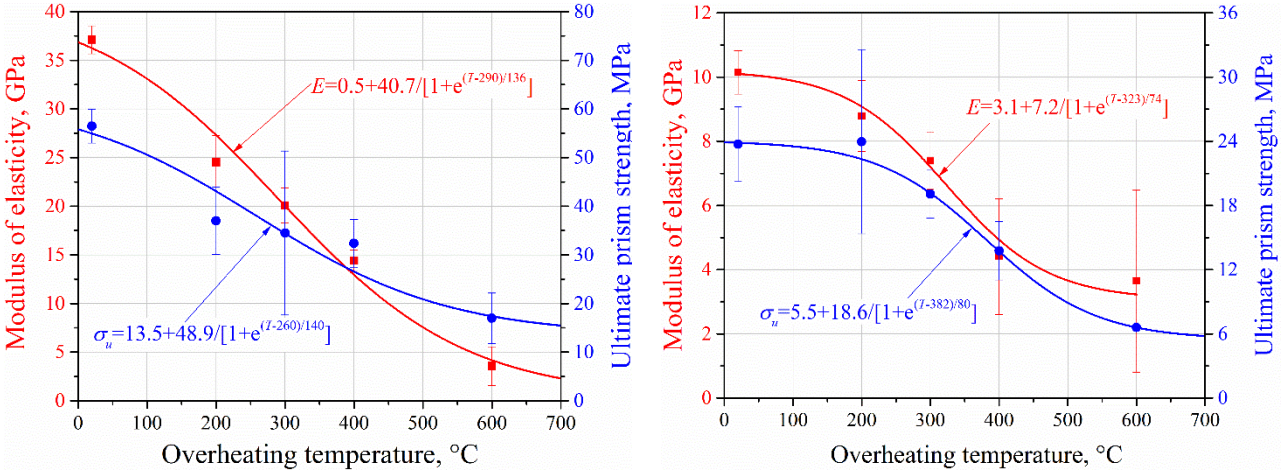

a) b)

Figure 6 Overheating temperature dependence of the elastic modulus and compressive strength for: a) Concrete 1 and b) Concrete 2

Constitutive equations

The three dimensional rate-independent elastic-plastic material model of concrete deformation with taking into account damage accumulation is considered. In order to capture the phenomenon of elastic stiffness degradation of the concrete as well as its irreversible deformations upon monotonic and cyclic loading, the combined use of elastic-plastic constitutive equations along with methods of continuum damage mechanics became vital to better describe the mechanical behavior of concrete. The damage growth is considered as a function of accumulated plastic strains in the coupled elastic-plastic-damage model [1–3].

The difference of the presented model from the elastic-damage and elastic-plastic models consists in the possibility of simultaneously taking into account the accumulation effect of residual strains and elastic stiffness degradation (see Fig. 7).

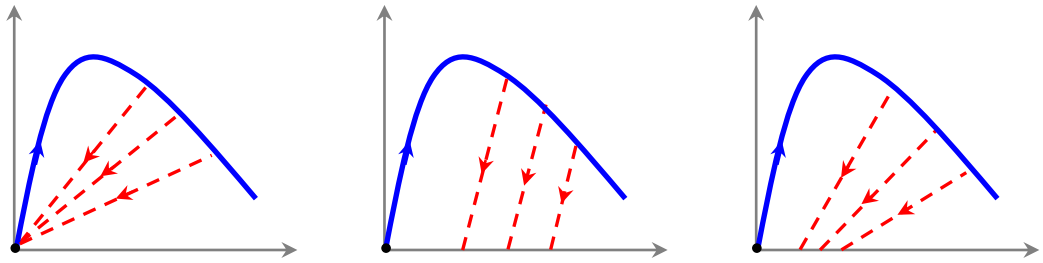

a) b) c)

Figure 7. Schematic representation of stress-strain curves with intermediate unloadings for: a) elastic-damage, b) elastic-plastic and c) elastic-plastic-damage models

The progressive propagation of microcracks plays a decisive role in the irreversible deformation of concrete, as it results in the elastic stiffness degradation. This effect is captured in the models by introducing of damage variables. In the simples case the influence of microcracking is introduced via a single scalar damage variable *D* ranging from 0 for the undamaged material to 1 for completely damaged material. The constitutive equations of material with scalar isotropic damage have been introduced by Kachanov [31] and further developed by Rabotnov [32] and others.

The constitutive equation of elastic-plastic material with scalar isotropic damage for three dimensional general multiaxial case takes the following form:

$$\boldsymbol{\sigma} = (1-D)\ {}^4\mathbf{C}_0^e \cdot\cdot (\boldsymbol{\varepsilon} - \boldsymbol{\varepsilon}^p) = {}^4\mathbf{C}^e \cdot\cdot (\boldsymbol{\varepsilon} - \boldsymbol{\varepsilon}^p), \tag{1}$$

where $\boldsymbol{\sigma}$ is Cauchy stress tensor, $\boldsymbol{\varepsilon}$ is the strain tensor, $\boldsymbol{\varepsilon}^p$ is the plastic strain tensor, ${}^4\mathbf{C}_0^e$ the initial (undamaged) elastic stiffness of the material, while ${}^4\mathbf{C}^e = (1-D)\ {}^4\mathbf{C}_0^e$ is the degraded elastic stiffness tensor. The effective stress tensor is defined by the relation:

$$\overline{\boldsymbol{\sigma}} = {}^4\mathbf{C}_0^{el} \cdot\cdot (\boldsymbol{\varepsilon} - \boldsymbol{\varepsilon}^p) = \frac{\boldsymbol{\sigma}}{1-D}, \tag{2}$$

Microcracking (under tension) and crushing (under compression) in concrete are represented by increasing values of the hardening (softening) variables. These variables control the evolution of the yield surface and the degradation of the elastic stiffness. The yield function represents a surface in effective stress space $F(\overline{\boldsymbol{\sigma}}, \tilde{\varepsilon}^p) \le 0$ which determines the states of failure or damage.

The evolution of the scalar degradation variable is defined by the function

$$D = D\left(\overline{\boldsymbol{\sigma}}, \tilde{\varepsilon}^p\right), \tag{3}$$

governed by a set of the effective stress tensor $\overline{\boldsymbol{\sigma}}$ and hardening (softening) variables $\tilde{\varepsilon}^p$. In the used in further Lubliner model [1], the stiffness degradation is initially isotropic and defined by degradation variable D_c in a compression zone and variable D_t in a tension zone. Total damage is defined as $D = 1-(1-D_c)(1-D_t)$. Damage states in tension and compression are characterized independently by two hardening variables $\tilde{\varepsilon}_t^p$ and $\tilde{\varepsilon}_c^p$, which are referred to equivalent plastic strains in tension and compression, respectively. The evolution of the hardening variables is given by the following expressions $\dot{\tilde{\varepsilon}}_t^p = r(\overline{\boldsymbol{\sigma}})\dot{\varepsilon}_1^{pl}$ and $\dot{\tilde{\varepsilon}}_c^p = -\left[1-r(\overline{\boldsymbol{\sigma}})\right]\dot{\varepsilon}_3^{pl}$, where $r(\overline{\boldsymbol{\sigma}}) = \sum_{i=1}^{3}\langle\overline{\sigma}_i\rangle / \sum_{i=1}^{3}|\overline{\sigma}_i|$, ε_1^{pl} and ε_3^{pl} are the maximum and minimum eigenvalues of the plastic strain tensor $\boldsymbol{\varepsilon}^p$; $\overline{\sigma}_1 \ge \overline{\sigma}_2 \ge \overline{\sigma}_3$ are the eigenvalues of the effective stress tensor $\overline{\boldsymbol{\sigma}}$ (2). The Macaulay brackets are defined as $\langle \mathrm{x} \rangle = \frac{1}{2}\left(|\mathrm{x}| + \mathrm{x}\right)$.

The plastic flow is governed by a flow potential function $G(\overline{\boldsymbol{\sigma}})$ according to non-associative flow rule:

$$\dot{\boldsymbol{\varepsilon}}^{p}=\begin{cases}\mathbf{0}, & F<0 \text{ or } F=0,\ \dot{F}<0;\\ \dot{\lambda}\dfrac{\partial G(\bar{\boldsymbol{\sigma}})}{\partial\bar{\boldsymbol{\sigma}}}, & F=0,\ \dot{F}=0;\end{cases} \quad (4)$$

where the loading function $F\left(\bar{\sigma},\tilde{\varepsilon}^{p}\right)\le 0$ is introduced for the description of the plastic flow onset and is defined by the expression generalized the Drucker-Prager yield condition [1]:

$$F=\frac{1}{1-\alpha}\left(\sqrt{3\bar{J}_2}+\alpha\bar{I}_1+\theta(\tilde{\varepsilon}^{p})\langle\bar{\sigma}_1\rangle-\gamma\langle-\bar{\sigma}_1\rangle\right)-\bar{\sigma}_c(\tilde{\varepsilon}_c^{p})=0, \quad (5)$$

where α and γ are material parameters; $-\bar{I}_1/3$ is the effective hydrostatic stress ($\bar{I}_1=\mathbf{1}\cdot\cdot\bar{\boldsymbol{\sigma}}$, where **1** is the unit tensor); $\sqrt{3\bar{J}_2}$ is the equivalent von Mises stress ($\bar{J}_2=\frac{1}{2}dev\bar{\boldsymbol{\sigma}}\cdot\cdot dev\bar{\boldsymbol{\sigma}}$), $dev\bar{\boldsymbol{\sigma}}=\bar{\boldsymbol{\sigma}}-\frac{1}{3}\mathbf{1}\bar{I}_1$ is the effective stress deviator. The shape of the loading surface on the deviator plane is determined by the parameter γ. The parameter $\alpha=\dfrac{f_{b0}/f_c-1}{2f_{b0}/f_c-1}$ is calculated from the Kupfer curve [33], where f_{b0}, f_c are the initial equibiaxial and uniaxial compressive yield stresses. The function $\theta(\tilde{\boldsymbol{\varepsilon}}^{p})$ is defined by the expression $\theta(\tilde{\varepsilon}^{p})=\dfrac{\bar{\sigma}_c(\tilde{\varepsilon}_c^{p})}{\bar{\sigma}_t(\tilde{\varepsilon}_t^{p})}(1-\alpha)-(1+\alpha)$ with $\bar{\sigma}_c,\bar{\sigma}_t$ being effective yield strength values at compression and tension. If a biaxial compression is applied with $\bar{\sigma}_1=0$, the Eq. (5) is reduced to the well-known Drucker-Prager yield condition. The shape of loading surface in the deviatoric plane is determined by the parameter $\gamma=\dfrac{3\left[1-\left(\sqrt{3\bar{J}_2}\right)_{TM}/\left(\sqrt{3\bar{J}_2}\right)_{CM}\right]}{2\left(\sqrt{3\bar{J}_2}\right)_{TM}/\left(\sqrt{3\bar{J}_2}\right)_{CM}+3}$, where indices TM and CM mean, respectively, the „Tensile Meridian" ($\sigma_1>\sigma_2=\sigma_3$) and the „Compressive Meridian" ($\sigma_1=\sigma_2>\sigma_3$) in the yield surface.

The plastic potential *G*, which is in general case different from *F*, sets the direction of the plastic flow in (4) and is defined by the expression generalizing the Drucker and Prager yield criterion [1]:

$$G=\sqrt{\left(f_c-m\cdot f_t\cdot\tan\beta\right)^2+3\bar{J}_2}+\tfrac{1}{3}\bar{I}_1\cdot\tan\beta, \quad (6)$$

where f_t and f_c are the uniaxial tensile and compressive strengths of concrete, respectively; β is the dilatation angle, measured in the plane $\frac{1}{3}\bar{I}_1-\sqrt{3\bar{J}_2}$ at high confining pressure; *m* is flow potential eccentricity, defining the slope of the potential asymptotic behavior.

Further improvements in the accuracy of model predictions can be achieved by using three-invariant loading function in form of the CAP model [34], ensuring the closed yield surfaces, and consideration of anisotropic damage tensor variables [35, 36].

Features of numerical implementation and optimal strategies for obtaining results of finite element modeling for this class of problems are considered in [5, 9, 19, 37].

Material parameter identification

The progressive elastic stiffness degradation from cycle to cycle provides information for the damage calculation. The damage (in compression) is considered as a scalar variable *D*, which is equal to 0 for virgin material and equal to 1 at the failure. As consequence of the equation $E=(1-D)E_0$ (valid under the hypothesis of strain equivalence) the damage variable at *k*-th cycle can be evaluated as:

$$D_k=1-E_k/E_0, \quad (7)$$

where E_0 is the value of the initial (undamaged) modulus and E_k is the values of the damaged moduli at the at *k*-th cycle. A typical example of calculation of the current elastic moduli based on a cyclic stress-strain curve for Concrete 2 at 20 °C (preliminarily overheated at 600 °C) is shown in Figure 8.

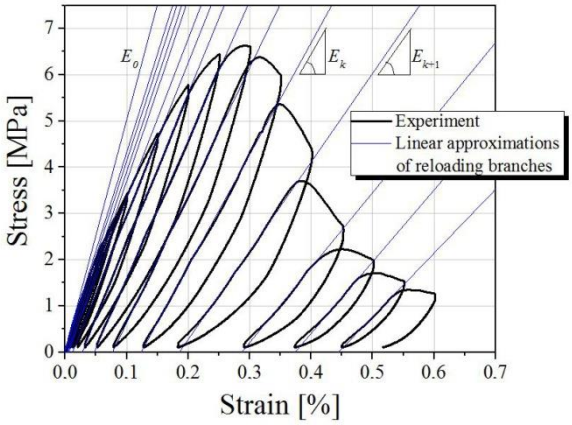

Figure 8. Illustration of the determination of the elastic reloading moduli of the damaged material (cyclic compression of Concrete 2 overheated at 600 °C)

Due to non-linear shape of both unloading and reloading branches of cyclic stress-strain curve it is a non-trivial problem to calculate appropriate elastic moduli of the damaged material. In the plasticity of metals, the current elastic modulus is determined by the tangential modulus at the beginning of the unloading or reloading curves (both are parallel). For the concrete this approach is not acceptable, the unloading and reloading curves are noticeably nonlinear and nonparallel. Therefore, we considered various (three-parametric family) methods for determining elastic modulus degradation based on using:

- different slope definition (tangent, secant, averaging);
- different branches of the cycle (unloading, reloading);
- different locations on the branch (tangent point or averaging range).

The secant slope is defined as an arc chord, connecting the beginning and the end of the branch. The averaging is performed within the branch (reloading (ascending) or unloading (descending)) or part of it. In this case the slope is identified for the selected group of points by the method of least squares.

In a comparative analysis 30 different methods are examined among them:

- 11 variants of tangent to reloading branch at 0%, 10%, 20%, ... , 90%, 100% of load;
- 11 variants of tangent to unloading branch at 0%, 10%, 20%, ... , 90%, 100% of load;
- 3 variants of averaging slope to reloading branch in ranges 0÷100%, 0÷10%, 90÷100% of load;
- 3 variants of averaging slope to unloading branch in ranges 0÷100%, 0÷10%, 90÷100% of load;
- secant slope (chord) of reloading branch in range 0÷100% of total load;
- secant slope (chord) of unloading branch in range 0÷100% of total load.

The following conditions are considered as criteria for the admissibility of the methods:

- $D > 0$ (the slope of E_k should be less than E_0);
- $D < 1$ (the slope of E_k should be greater than 0);
- monotonic decreasing elastic modulus with plastic deformation, or that is equivalent, monotonic increasing damage from cycle to cycle;
- condition of the possibility of strain localization [38];
- visually, the change in slope should correspond to the observed evolution of hysteresis loops.

For validation of the slope determination methods the obtained experimental cyclic stress-strain curves for Concrete 1, 2, 3 under various heat treatment conditions were used.

The results comparison of the tangents slopes for a representative cycle for Concrete 2 overheated at the temperature of 600 °C are shown in Figure 9. The tangents to the unloading branch shows a significantly larger scatter than the tangents to the reloading curve. The tangential modulus at the beginning of the unloading or reloading curves can't be considered as an adequate approximation of the slope. Appropriate slope approximations are obtained for tangents to reloading branch in the range 20÷60 % of total load for the considered cycle (see also Fig. 10).

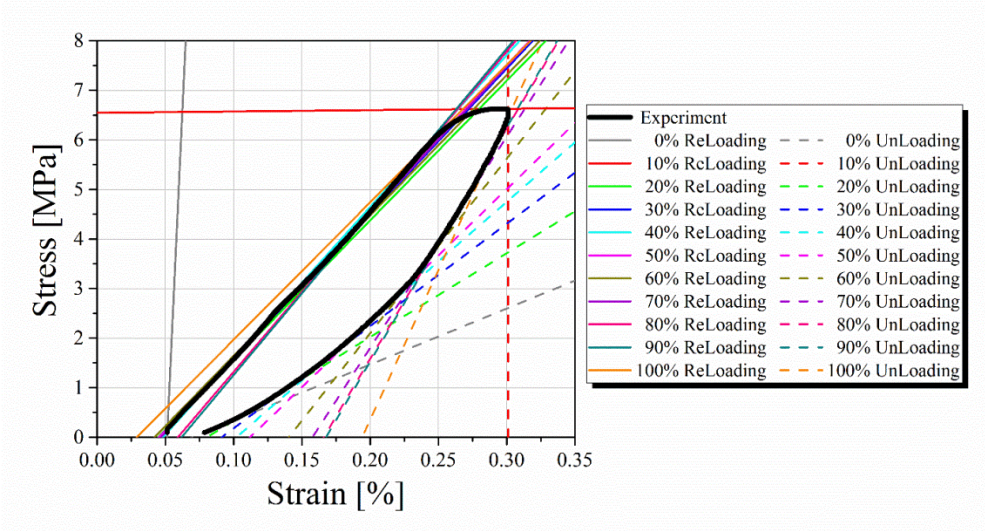

Figure 9. Comparison of tangents slopes for a representative compressive cycle for Concrete 2 overheated at 600 °C

A comparison of all 30 methods for the considering cycle is shown in Figure 10. The results of multivariant computations for the considering cycle and also for others cycles and for others considered concretes show that the averaging slopes in the ranges 0÷100 % and 0÷10 % to reloading branch as well as tangents in the range 20÷60 % to reloading branch provide the best variant of approximation. The range of unallowable damage values is indicated by red shading. The curves, visually corresponding to the slope of the hysteresis loop, are marked with a shaded green area. As a rule, outside this region, there is a lack of monotony (oscillations) in the dependence of the elasticity modulus and damage with the growth of plastic strain.

For the convenience of visual comparison, the most characteristic variants are presented on one graph in Figure 11 for the same hysteresis loop as in Fig. 9 in the form of lines emanating from one point.

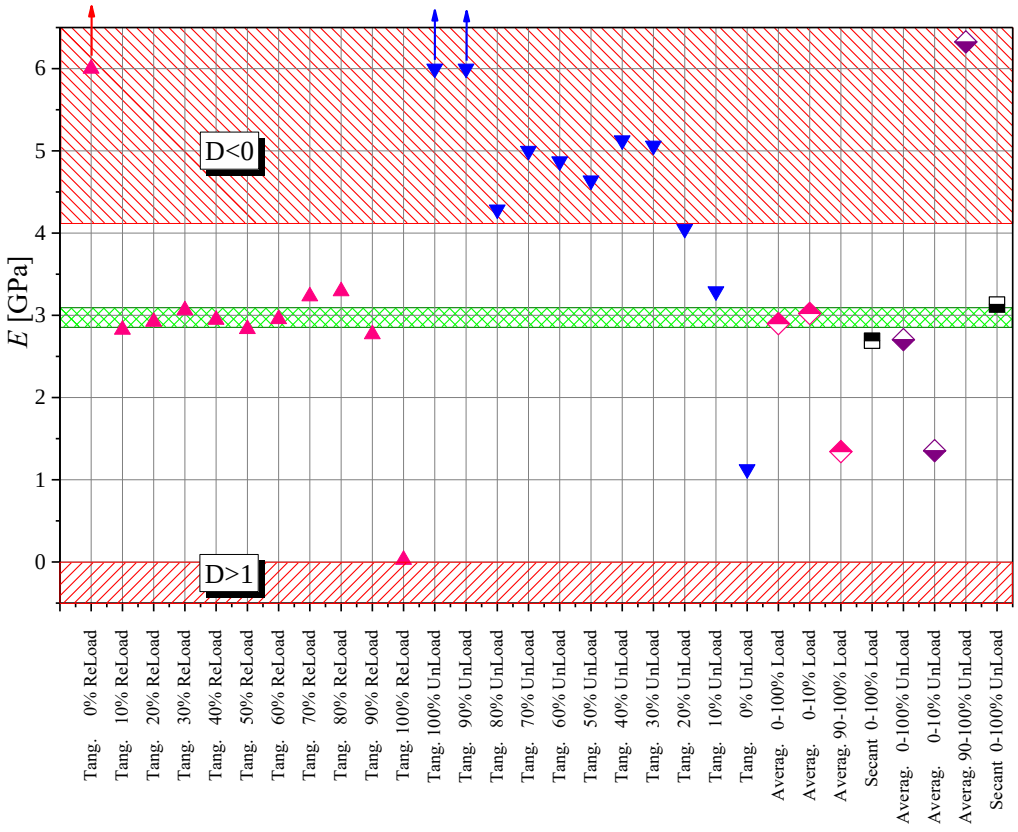

Figure 10. Comparison of slope predictions for a representative compressive cycle for Concrete 2 overheated at 600 °C

Benin A.V., Semenov A.S., Semenov S.G., Beliaev M.O., Modestov V.S. Methods of identification of concrete elastic-plastic-damage models. *Magazine of Civil Engineering*. 2017. No. 8. Pp. 279–297. doi: 10.18720/MCE.76.24.

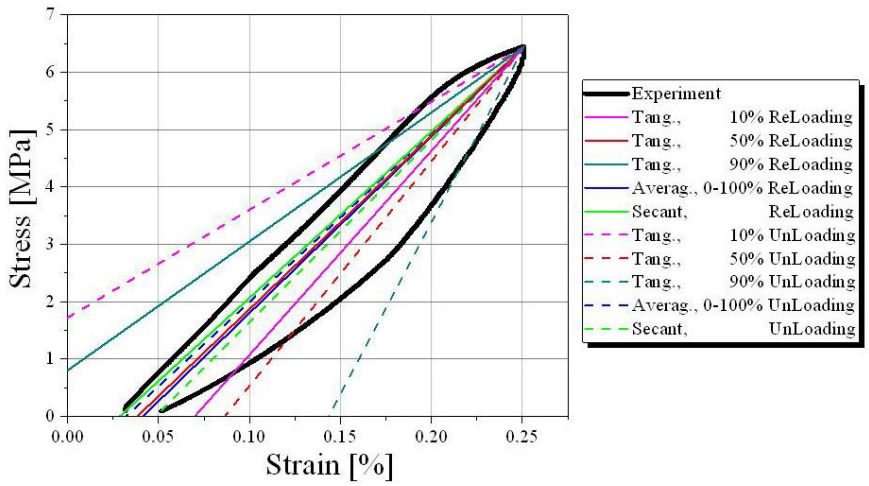

Figure 11. Comparison of tangents slopes for a representative compressive cycle for Concrete 2 overheated at 600 °C

The accuracy of the calculation of the damage affects the accuracy of the definition of plastic strain, which is determined in uniaxial case by the equation:

$$\varepsilon^p = \varepsilon - \frac{\sigma}{E} = \varepsilon - \frac{\sigma}{(1-D)E_0}. \tag{8}$$

When specifying the input data in ABACUS, inelastic strain is also used, which is determined as

$$\varepsilon^{in} = \varepsilon - \frac{\sigma}{E_0} = \varepsilon - \frac{(1-D)\sigma}{E}. \tag{9}$$

The relationship between plastic and inelastic deformations can be obtained by the total strain decomposition $\boldsymbol{\varepsilon} = \boldsymbol{\varepsilon}^e + \boldsymbol{\varepsilon}^p = \boldsymbol{\varepsilon}^{e0} + \boldsymbol{\varepsilon}^D + \boldsymbol{\varepsilon}^p = \boldsymbol{\varepsilon}^{e0} + \boldsymbol{\varepsilon}^{in}$ and written in the form:

$$\varepsilon^p = \varepsilon^{in} + \frac{\sigma}{E_0} - \frac{\sigma}{(1-D)E_0} = \varepsilon^{in} - \frac{D\sigma}{(1-D)E_0}. \tag{10}$$

The results of elastic moduli degradation and damage calculation as function of plastic strain under compression are given in Fig. 12 for Concrete 1 (non-overheated) and Concrete 2 (overheated at 600º).

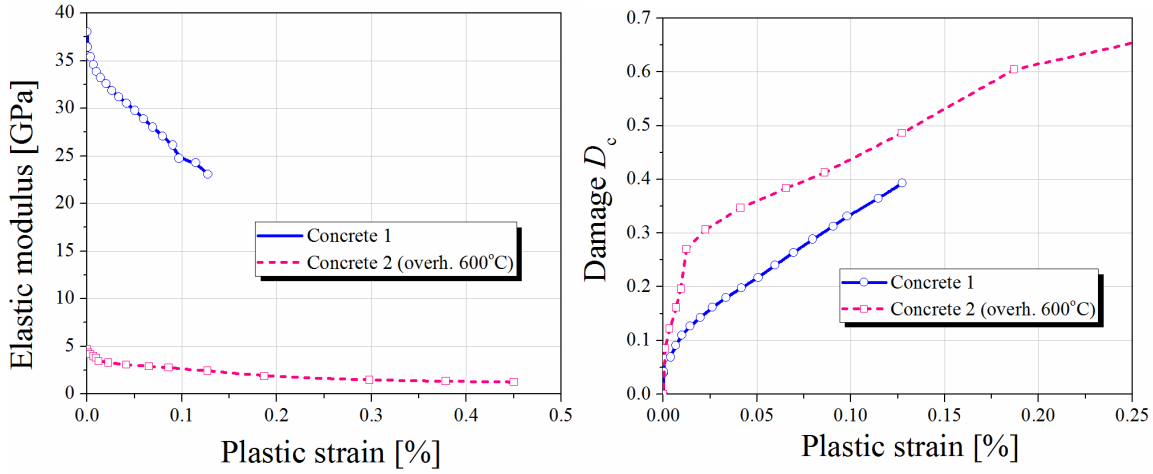

a) **b)**

Figure 12. Elastic modulus degradation (a) and damage evolution (b) with increasing of plastic strain for regular and overheated at 600o Concrete 2 under compression

Бенин А.В., Семенов А.С., Семенов С.Г., Беляев М.О., Модестов В.С. Методы идентификации упруго-пластических моделей бетона с учетом накопления повреждений // Инженерно-строительный журнал. 2017. № 8(76). С. 279–297.

Comparison of obtained results of damage evolution with experimental data from literature [21-28] are given in Fig. 13. Damage evolution curves are obtained on the base stress-strain curves, which are shown in Figs. 1a, 1b, 4a, 4d, 8. Dependences of the damage on the dimensionless (by the peak value) strain show close monotonic increasing results both in tension and compression. Inflection point in the damage curve for overheated at 600° Concrete 2 is observed at strain peak that corresponds also to the experimental data for overheated concretes considered in [15].

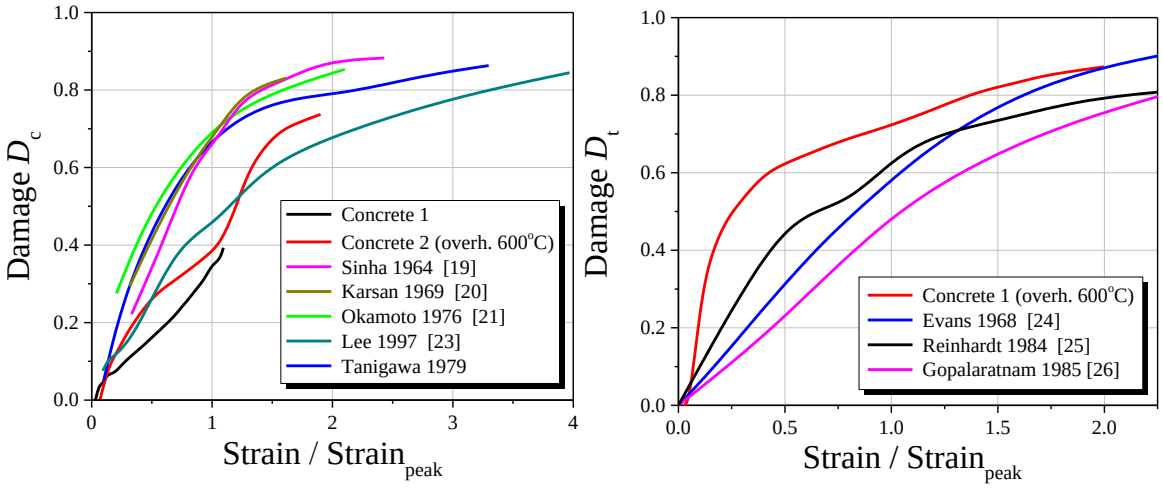

a) **b)**

Figure 13. Damage evolution under: a) compression and b) tension for various concretes

The exponential approximation [3,6,19,37] can be considered as the simplest approximation of the damage curve:

$$D = 1 - e^{-b\varepsilon}, \tag{11}$$

where *b* is a material constant. An example of a more complex approximation, which allows to more accurately take into account the shape of the curve, is the following expression [39]:

$$D = \begin{cases} 0, & \varepsilon < \varepsilon_0, \\ 1 - e^{-b(\varepsilon - \varepsilon_0)^g}, & \varepsilon \geq \varepsilon_0, \end{cases} \tag{12}$$

where material constant *b* rules how fast *D* approaches 1, *g* is a shape parameter, ε_0 introduces a threshold value.

It is obvious that the compressive and tensile constants must be different.

Note that the experimental data shown in Figure 13 do not allow us to identify the appearance of a clearly expressed threshold greater than 0.2 ε_{peak}.

Validation and verification

Comparison of simulation results with experimental data for samples

The comparison of simulation results with experimental data under monotonic compression for regular Concrete 1 and for overheated at 600 °C Concrete 2 are given in Figure 14. A good agreement is observed in both cases. The model parameters are identified with help of the relations (7) and (10). The constitutive equations (1)-(6) are used in simulations. Note that the considered approach allows to describe strain hardening, softening and post-peak behavior under compression and tension. An example of material constants used in simulations for regular Concrete 1 at 20 °C is given in Table 1.

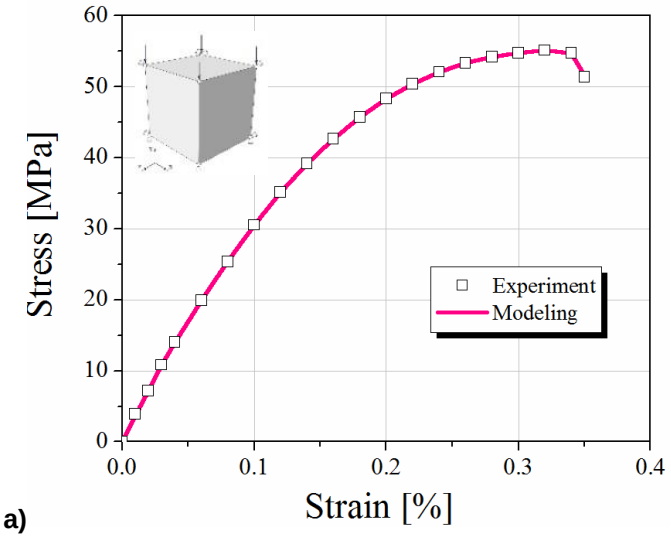

a)

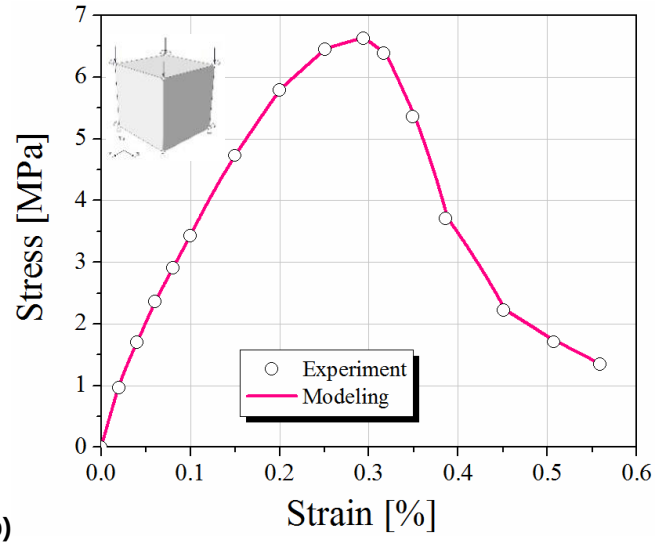

b)

Figure 14. Comparison of simulation results with experimental data under compression for regular Concrete 1 (a) and for overheated at 600 oC Concrete 2 (b)

The validation results of proposed identification procedure under cyclic loading for regular and for overheated concrete are given in Figure 15. Prediction accuracy is lower in comparison with monotonic case, but a satisfactory agreement of experiment and simulation results is observed in this case too.

The considered model is limited by the possibility to predict only the linear unloading. This reduces the accuracy of the computations. One of the possible ways to further improve the material model is to consider structural or multisurface models.

Table 1. Material constants for regular Concrete 1 used in simulations of monotonic and cyclic loading of samples

E [GPa]	v [-]	β [º]	$\frac{f_{b0}}{f_{c0}}$	σ_c^{peak} [MPa]	ε_c^{peak} [%]	σ_t^{peak} [MPa]	ε_t^{peak} [%]
38	0.2	38	1.12	-55.1	-0.32	2.77	0.035

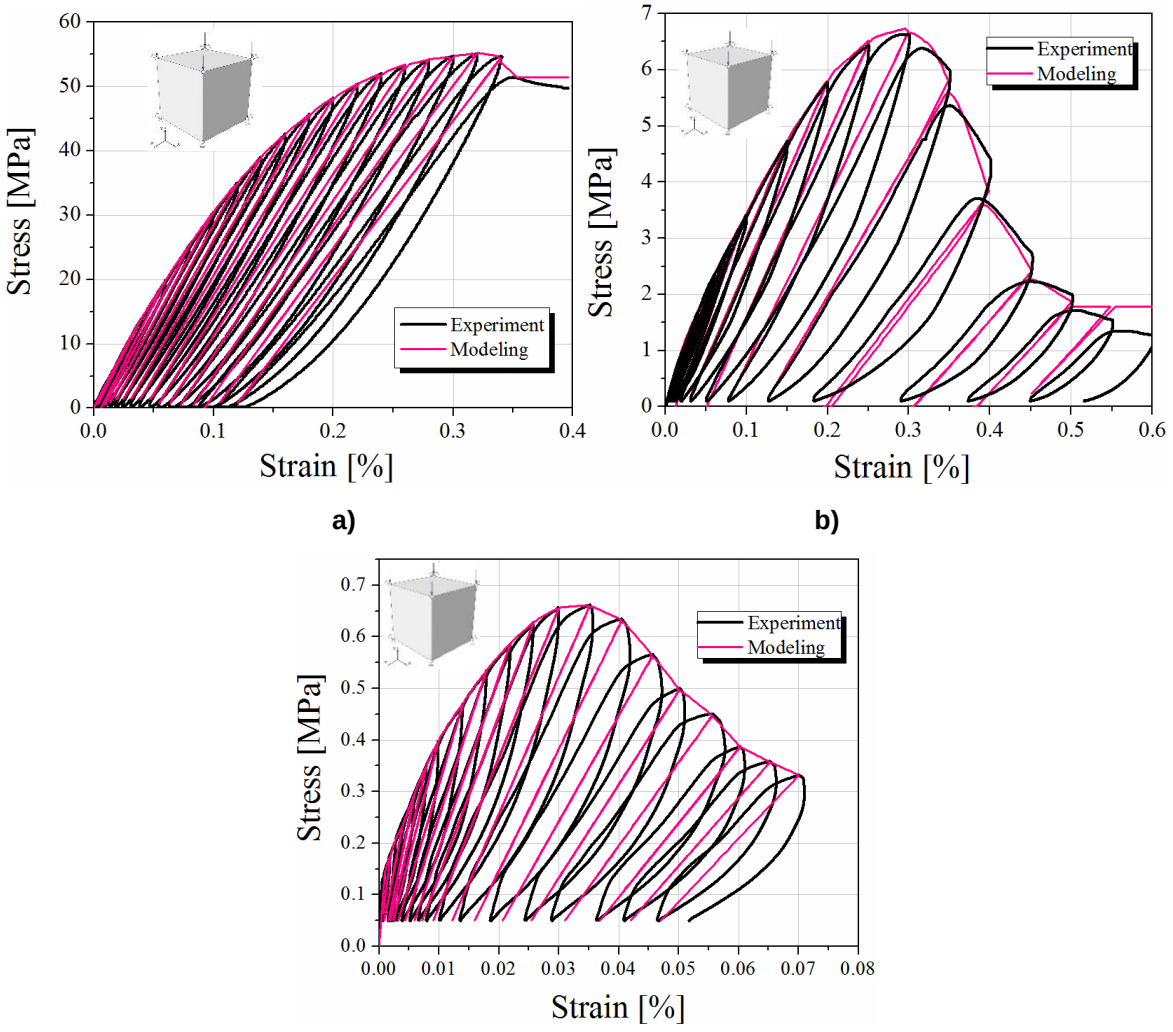

Figure 15. Comparison of simulation results with experimental data for cyclic loading:
a) compression for regular Concrete 1;
b) compression for overheated at 600 °C Concrete 2;
c) tension for overheated at 600 °C Concrete 1

Pulling the reinforcing bar from the concrete block

A direct finite element modeling of the pulling process of the steel reinforcing bar out from the concrete block (in accordance with RILEM/CEB/FIB [40] requirements) with using the elastic-plastic-damage constitutive equations (1)–(6) for the concrete and with taking into account the cohesive behavior of steel-concrete bond is considered.

Geometric parameters, pull-out test experiment (used tensile tester Shimadzu AG-300kN) and axisymmetrical finite-element model are shown in Figures 16 a-c. Material constants used in finite-element simulations are listed in Table 2. A detailed description of the problem and an analysis of the results are given in [41, 11, 12]. Damage field distributions are shown in Figures 16d and e. The damage localization is observed in the vicinity of the reinforcing rod-to-concrete contact.

The comparison of obtained results of finite element simulations with experimental data for the problem of pulling the reinforcing bar from the concrete block demonstrates a good agreement (see Fig. 16f). The proposed approach, which is based on direct FE modeling of reinforced concrete elements with account of elastic-plastic-damage material model of concrete in combination with taking into account cohesive behavior for interface between reinforcement and concrete, allows to describe correctly reinforced-concrete bond at pulling the rod out of the concrete body.

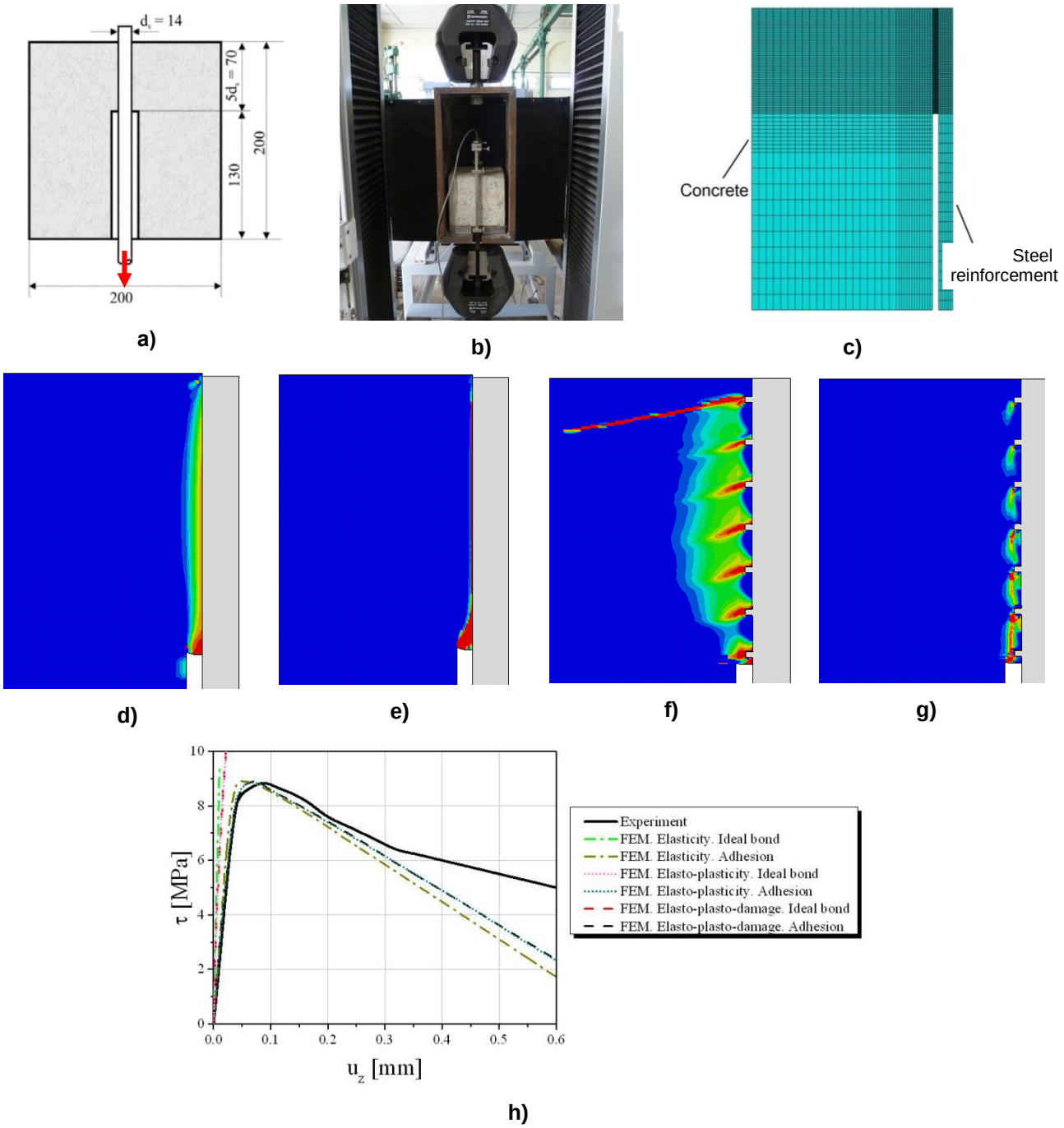

Figure 16. Pull-out test: a) specimen geometry; b) test setup; c) finite-element model; d) damage at tension D_t (model with account of reinforcement ribs); e) damage at compression D_c (model with account of ribs); f) damage at tension D_t (model without account of ribs); g) damage at compression D_c (model without account of ribs); h) shear stress in bond τ vs displacement of reinforcement u_z for various models

Table 2. Concrete material constants used in simulation of pulling the reinforcing bar from the concrete block

E [GPa]	v [-]	β [º]	$\frac{f_{b0}}{f_{c0}}$	σ_c^{peak} [MPa]	ε_c^{peak} [%]	σ_t^{peak} [MPa]	ε_t^{peak} [%]
30	0.2	38	1.12	-18.5	-0.136	1.55	0.0403

Бенин А.В., Семенов А.С., Семенов С.Г., Беляев М.О., Модестов В.С. Методы идентификации упруго-пластических моделей бетона с учетом накопления повреждений // Инженерно-строительный журнал. 2017. № 8(76). С. 279–297.

Three-point bending of reinforced concrete beam

Finite-element simulation of the fracture process of the reinforced concrete straight beam (Fig. 17) of rectangular cross-section with longitudinal reinforcement under a three-point bending with using of the elastic-plastic-damage constitutive equations (1)–(6) for the concrete is considered.

Geometric parameters, three-point bending experiment (used Instron 1200 KN series SATEC™) and finite-element model (one-fourth of the specimen due to symmetry) are shown in Figure 17a-c. Material properties are listed in Table 3. Maximum principal strain and damage field distributions are shown in Figures 17e and f. The zones of strain and damage localizations are in an agreement with the macrocracks locations and orientations observed in the experiments (Fig. 17d).

The comparison of obtained results of finite element simulations for displacements with experimental data demonstrates a good agreement (see Fig. 17g).

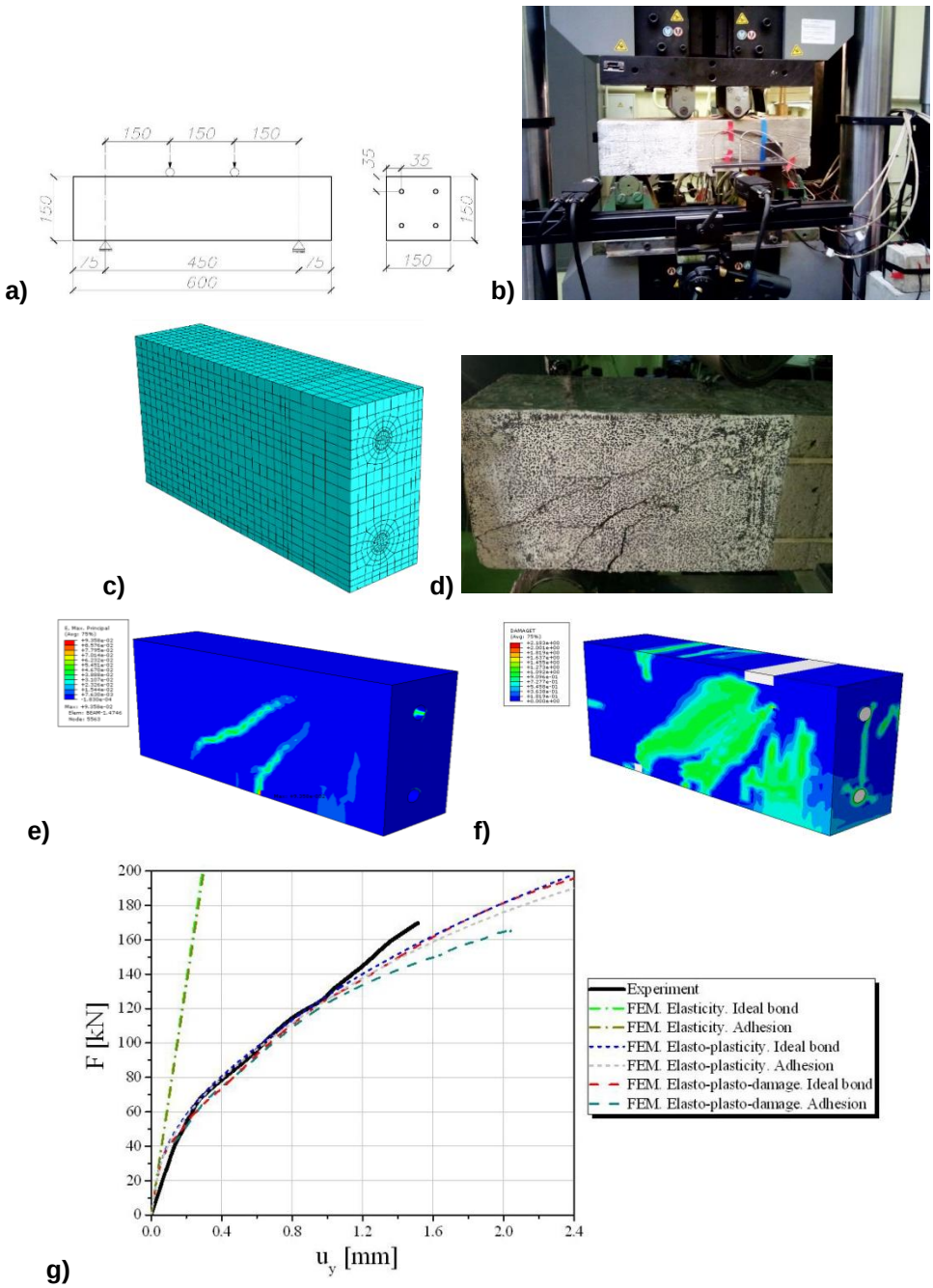

Figure 17. Three-point bending of reinforced concrete beam: a) specimen geometry; b) test setup; c) finite-element model; d) specimen after fracture, e) maximum principal strain; f) damage at tension Dt; g) load vs displacement of the bottom point of the central section of the concrete beam for various models

Benin A.V., Semenov A.S., Semenov S.G., Beliaev M.O., Modestov V.S. Methods of identification of concrete elastic-plastic-damage models. *Magazine of Civil Engineering*. 2017. No. 8. Pp. 279–297. doi: 10.18720/MCE.76.24.

Table 3. Concrete material constants used in simulation of three-point bending of reinforced concrete beam

E [GPa]	v [-]	β [º]	$\frac{f_{b0}}{f_{c0}}$	σ_c^{peak} [MPa]	ε_c^{peak} [%]	σ_t^{peak} [MPa]	ε_t^{peak} [%]
34.5	0.2	38	1.12	-25.5	-0.163	1.95	0.0441

Examples of other applications of the considered elastic-plastic-damage model in solving real problems of practice, such as corrosion driven spalling of concrete cover at automobile bridge [42] and simulation of fracture process of ballastless deck at railway bridge [13] have been also demonstrated the possibility of applying the considered approach.

Conclusion

The material parameter identification procedure of elastic-plastic-damage concrete model is proposed and validated. The results of multivariant calculations of damage on the base of experimental cyclic stress-strain curves under tension and compression show that the averaging slopes of reloading branch as well as tangents in the middle of reloading branch provide the best variant of approximation. Comparison of simulation results with experimental data under monotonic and cyclic compression demonstrates a good agreement for regular and for overheated concrete. Additional indirect verification of the considered material model and the proposed methods for identifying its parameters is the good accuracy of the simulation results in comparison with the results of the experiments when solving real practical problems, such as the pulling the reinforcing bar from the concrete block and three-point bending of reinforced concrete beam. The offered approach, which is based on direct three-dimensional modeling of reinforced concrete structures with account of continuum damage evolution, allows to describe inelastic deformation, define cracking mechanisms and to evaluate a residual resource of partially destroyed structures. However, practical realization of this approach requires considerable computational effort and additional experimental data concerning concrete mechanical properties.

Reference

1. Lubliner J., Oliver J., Oller S., Oñate E. A Plastic-Damage Model for Concrete. *Int. Journal of Solids and Structures*. 1989. No. 3(25). Pp. 229–326.
2. Voyiadjis G.Z., Abu Lebdeh T.M. Plasticity model for concrete using the bounding surface concept. *Int. J. Plast.* 1994. No. 10(1). Pp. 1–21.
3. Lee J., Fenves G.L. Plastic-damage model for cyclic loading of concrete structures. *Journal of Engineering Mechanics.* 1998. No. 124(8). Pp. 892–900.
4. Kratzig W.B., Pölling R. An elasto-plastic damage model for reinforced concrete with minimum number of material parameters. *Computers and Structures.* 2004. No. 82(15–16). Pp. 1201–1215.
5. Jason L., Huerta A., Pijaudier-Cabot G., Ghavamian, S. An elastic plastic damage formulation for concrete: Application to elementary tests and comparison with an isotropic damage model. *Computer Methods in Applied Mechanics and Engineering.* 2006. No. 195(52). Pp. 7077–7092.
6. Grassl P., Jirasek M. Damage-plastic model for concrete failure. *International Journal of Solids and Structures.* 2006. No. 43. Pp. 7166–7196.
7. Mazars J., Pijaudier-Cabot G. Continuum damage theory-Application to concrete. *Journal of Engineering Mechanics.* 1989. No. 115(2). Pp. 345–365.
8. Voyiadjis G.Z., Taqieddin Z.N. Elastic plastic and damage model for concrete materials: part i - theoretical formulation. *International Journal of Structural Changes in Solids – Mechanics and Appl.* 2009. No. 1(1). Pp. 31–59.
9. ABAQUS User's manual, ver. 6.12 Abaqus Inc.; 2012.
10. Benin A.V., Semenov A.S., Semenov S.G. Fracture simulation of reinforced concrete structure with account of bond degradation and concrete cracking under steel corrosion. *Advances in Civil Engineering and Building Materials. Proc. 2nd Int. Conf. on Civil Eng. and Building Materials.* 2012. Taylor & Francis Group, London.

Литература

1. Lubliner J., Oliver J., Oller S., Oñate E. A plastic-damage model for concrete // Int. Journal of Solids and Structures. 1989. № 3(25). Pp. 229–326.
2. Voyiadjis G.Z., Abu Lebdeh T.M. Plasticity model for concrete using the bounding surface concept // Int. J. Plast. 1994. № 10(1). Pp. 1–21.
3. Lee J., Fenves G.L. Plastic-damage model for cyclic loading of concrete structures // Journal of Engineering Mechanics. 1998. № 124(8). Pp. 892–900.
4. Kratzig W.B., Pölling R. An elasto-plastic damage model for reinforced concrete with minimum number of material parameters // Computers and Structures. 2004. № 82(15–16). Pp. 1201–1215.
5. Jason L., Huerta A., Pijaudier-Cabot G., Ghavamian, S. An elastic plastic damage formulation for concrete: Application to elementary tests and comparison with an isotropic damage model // Computer Methods in Applied Mechanics and Engineering. 2006. № 195(52). Pp. 7077–7092.
6. Grassl P., Jirasek M. Damage-plastic model for concrete failure // International Journal of Solids and Structures. 2006. № 43. Pp. 7166–7196.
7. Mazars J., Pijaudier-Cabot G. Continuum damage theory-Application to concrete // Journal of Engineering Mechanics. 1989. № 115(2). Pp. 345–365.
8. Voyiadjis G.Z., Taqieddin Z.N. Elastic plastic and damage model for concrete materials: Part I - Theoretical Formulation // International Journal of Structural Changes in Solids – Mechanics and Appl. 2009. № 1(1). Pp. 31–59.
9. ABAQUS User's manual, ver. 6.12 Abaqus Inc.; 2012.
10. Benin A.V., Semenov A.S., Semenov S.G. Fracture simulation of reinforced concrete structure with account of bond degradation and concrete cracking under steel corrosion // Advances in Civil Engineering and Building Materials. Proc. 2nd Int. Conf. on Civil Eng. and Building Materials. 2012. Taylor & Francis Group, London.

Бенин А.В., Семенов А.С., Семенов С.Г., Беляев М.О., Модестов В.С. Методы идентификации упруго-пластических моделей бетона с учетом накопления повреждений // Инженерно-строительный журнал. 2017. № 8(76). С. 279–297.

Pp. 233–237.
11. Benin A.V., Semenov A.S., Semenov S.G., Melnikov B.E. Simulation of degradation of bond between reinforcing bar and concrete. Part 1. Models with account of the discontinuity. *Magazine of Civil Engineering.* 2013. No. 5(40). Pp. 86-99. (rus)
12. Benin A.V., Semenov A.S., Semenov S.G., Melnikov B.E. The simulation of bond fracture between reinforcing bars and concrete. Part 2. Models without taking the bond discontinuity into account. *Magazine of Civil Engineering.* 2014. No. 1 (45). Pp. 23–40. (rus)
13. Benin A.V., Semenov A.S., Semenov S.G. Fracture analysis of reinforced concrete bridge structures with account of concrete cracking under steel corrosion. *Advanced Materials Research.* 2014. No. 831. Pp. 364–369.
14. Jankowiak T., Lodygowski T. Identification of parameters of concrete damage plasticity constitutive model. *Found. Civ. Environ. Eng.* 2005. No 6. Pp. 53–69.
15. Neuenschwander M., Knobloch M., Fontana M. Suitability of the damage-plasticity modelling concept for concrete at elevated temperatures: Experimental validation with uniaxial cyclic compression tests. *Cem. Concr. Res.* 2016. No. 79. Pp. 57–75.
16. Gajewski T., Garbowski T. Calibration of concrete parameters based on digital image correlation and inverse analysis. *Archives of Civil and Mechanical Engineering*. 2014. No. 1(14). Pp. 170–180.
17. Barashikov A.Ia. *Raschet zhelezobetonny`kh konstruktcii` na dei`stvie dlitel`ny`kh peremenny`kh nagruzok* [Structural analysis of reinforced concrete structures under permanently acting loads]. Kiev: Budivel`nik, 1977. 156 p. (rus)
18. Barashikov A.Ia., Shevchenko B.A., Valovoi` A.I. Malotciclovaia vy`noslivost` betona pri szhatii [Low-cycle fatigue of concrete under pressure]. *Beton i zhelezobeton.* 1985. No. 4. Pp. 27–28. (rus)
19. Nechnech W., Meftah F., Reynouard J.M. An elasto-plastic damage model for plain concrete subjected to high temperatures. *Engineering Structures*. 2002. No. 24. Pp. 597–611.
20. *Russian State Standard GOST 10180-12* Concretes. Methods for strength determination using reference specimens. 2013. 30 p. (rus)
21. Sinha B.P., Gerstle. K.H., Tulin.L.G. Stress-strain relations for concrete under cyclic loading. *ACI J Proc.* 1964. No. 61(2). Pp. 195–211.
22. Karsan I.D., Jirsa J.O. Behavior of concrete under compressive loading. *Journal of the Structural Division*. 1969. No. 95(ST12). Pp. 2543–2563.
23. Okamoto S., Shiomi S., Yamabe K. Earthquake resistance of prestressed concrete structures. *Proceedings of Annual Architectural Instititute of Japan*. 1976. Pp. 1251–1252.
24. Mazars J., Berthaud Y., Ramtani S. The unilateral behavior of damaged concrete. *Engineering Fracture mechanics.* 1990. No. 35(4). Pp. 629–635.
25. Lee Y.-H., Willam K. Mechanical properties of concrete in uniaxial compression. *ACI Materials Journal.* 1997. No. 94(6). Pp. 457–471.
26. Evans R.H., Marathe M.S. Microcracking and stress-strain curves for concrete in tension. *Materials and Structures*. 1968. No. 1(1). Pp. 61–64.
27. Reinhardt H.W. Fracture mechanics of an elastic softening material like concrete. *HERON.* 1984. No. 29(2). Pp. 3–41.
28. Gopalaratnam V.S., Shah S.P. Softening response of plain concrete in direct tension. *ACI Journal proceedings.* 1985. No. 82(3). Pp. 310–323.
29. Taerwe L.R. Influence of steel fibers on strain-softening of high-strength concrete. *ACI Mater J.* 1993.No. 89(1). Pp. 54–60.
30. Osorio E., Bairan J.M., Marı A.R. Lateral behavior of concrete under uniaxial compressive cyclic loading. *Materials and Structures.* 2013. No. 46. Pp. 709–724.

Pp. 233–237.
11. Бенин А.В., Семенов А.С., Семенов С.Г., Мельников Б.Е. Математическое моделирование процесса разрушения сцепления арматуры с бетоном. Часть 1. Модели с учетом несплошности соединения // Инженерно-строительный журнал. 2013. № 5(40). С. 86–99.
12. Бенин А.В., Семенов А.С., Семенов С.Г., Мельников Б.Е. Математическое моделирование процесса разрушения сцепления арматуры с бетоном. Часть 2. Модели без учета несплошности соединения // Инженерно-строительный журнал. 2014. № 1(45). С. 23–40
13. Benin A.V., Semenov A.S., Semenov S.G. Fracture analysis of reinforced concrete bridge structures with account of concrete cracking under steel corrosion // Advanced Materials Research. 2014. № 831. Pp. 364–369.
14. Jankowiak T., Lodygowski T. Identification of parameters of concrete damage plasticity constitutive model // Found. Civ. Environ. Eng. 2005. Vol. 6(1). Pp. 53–69.
15. Neuenschwander M., Knobloch M., Fontana M. Suitability of the damage-plasticity modelling concept for concrete at elevated temperatures: Experimental validation with uniaxial cyclic compression tests // Cem. Concr. Res. 2016. № 79. Pp. 57–75.
16. Gajewski T., Garbowski T. Calibration of concrete parameters based on digital image correlation and inverse analysis // Archives of Civil and Mechanical Engineering. 2014. № 1(14). Pp. 170–180.
17. Барашиков А.Я. Расчет железобетонных конструкций на действие длительных переменных нагрузок. Киев: Будивельник, 1977. 156 с.
18. Барашиков А.Я., Шевченко Б.А., Валовой А.И. Малоцикловая выносливость бетона при сжатии // Бетон и железобетон. 1985. № 4. С. 27–28.
19. Nechnech W., Meftah F., Reynouard J.M. An elasto-plastic damage model for plain concrete subjected to high temperatures // Engineering Structures. 2002. № 24. Pp. 597–611.
20. ГОСТ 10180-12 Бетоны. Методы определения прочности по контрольным образцам. 2013. 30 с.
21. Sinha B.P., Gerstle. K.H., Tulin.L.G. Stress-strain relations for concrete under cyclic loading // ACI J Proc. 1964. № 61(2). Pp. 195–211.
22. Karsan I.D., Jirsa, J.O. Behavior of concrete under compressive loading // Journal of the Structural Division. 1969. № 95(ST12). Pp. 2543–2563.
23. Okamoto S., Shiomi S., Yamabe K. Earthquake resistance of prestressed concrete structures // Proceedings of Annual Architectural Instititute of Japan. 1976. Pp. 1251–1252.
24. Mazars J., Berthaud Y., Ramtani S. The unilateral behavior of damaged concrete // Engineering Fracture mechanics. 1990. № 35(4). Pp. 629–635.
25. Lee Y.-H., Willam, K. Mechanical properties of concrete in uniaxial compression // ACI Materials Journal. 1997. № 94(6). Pp. 457–471.
26. Evans R.H., Marathe M.S. Microcracking and stress-strain curves for concrete in tension // Materials and Structures. 1968. № 1(1). Pp. 61–64.
27. Reinhardt H.W. Fracture mechanics of an elastic softening material like concrete // HERON. 1984. № 29(2). Pp. 3–41.
28. Gopalaratnam V.S., Shah S.P. Softening response of plain concrete in direct tension // ACI Journal proceedings. 1985. № 82(3). Pp. 310–323.
29. Taerwe L.R. Influence of steel fibers on strain-softening of high-strength concrete // ACI Mater J. 1993. № 89(1). Pp. 54–60.
30. Osorio E., Bairan J.M., Marı A.R. Lateral behavior of concrete under uniaxial compressive cyclic loading // Materials and Structures. 2013. № 46. Pp. 709–724.
31. Качанов Л.М. О времени разрушения в условиях ползучести // Известия АН СССР. Отд-ние техн. наук. 1958. № 8. С. 26–31.

Benin A.V., Semenov A.S., Semenov S.G., Beliaev M.O., Modestov V.S. Methods of identification of concrete elastic-plastic-damage models. *Magazine of Civil Engineering*. 2017. No. 8. Pp. 279–297. doi: 10.18720/MCE.76.24.

31. Kachanov L.M. O vremeni razrusheniya v usloviyakh polzuchesti [On the creep-rapture life]. *Izv. AN SSSR. Ser. Techn. Sci.* 1958. No. 8. Pp. 26–31. (rus)
32. Rabotnov Yu.N. O mekhanizme dlitelnogo razrusheniya [On the delayed fracture mechanics]. *Voprosy prochnosti materialov i konstruktsiy*. Moscow, AN SSSR. 1959. Pp. 5–7. (rus)
33. Kupfer H., Hilsdorf H.K., Rusch H. Behavior of concrete under biaxial stress. *Journal of the American Concrete Institute.* 1969. No. 66. Pp. 656–666.
34. Schwer L.E., Murry Y.D. A three-invariant smooth cap model with mixed hardening. *Int. J. for Num. Anal. Mech. In Geomech.* 1994. No. 18. Pp. 657–688.
35. Voyiadjis G.Z., Taqieddin Z.N., Kattan P.I. Anisotropic damage–plasticity model for concrete. *Int. Journal of Plasticity.* 2008. No. 10(24). Pp. 1946–1965.
36. Semenov A.S. Symmetrization of the effective stress tensor for anisotropic damaged continua. *St. Petersburg State Polytechnical University Journal. Physics and Mathematics.* 2017. No. 2(10). (rus)
37. Abu Al-Rub R.K., Kim S.-M. Computational applications of a coupled plasticity-damage constitutive model for simulating plain concrete fracture. *Engineering Fracture Mechanics.* 2010 No. 10(77). Pp. 1577–1603.
38. Beliaev M.O., Semenov A.S. Lokalizatsiia deformatsii pri chetyrekhtochechnom izgibe armirovannoi betonnoi balki [Strain localization under four-point bending of a reinforced concrete beam]. *Materialy Nauchnogo foruma s mezhdunarodnym uchastiem. Nedelia nauki SPbPU* [Proceedings of Scientific forum with international participation: Science Week SPbPU]. *2*015. Pp. 60–62. (rus)
39. Häussler-Combe U., Hartig J. Formulation and numerical implementation of a constitutive law for concrete with strain-based damage and plasticity. *International Journal of Non-Linear Mechanics.* 2008. No. 43. Pp. 399–415.
40. *RILEM/CEB/FIB.* Recommendation on reinforcement steel for reinforced concrete. RC6. Bond test for reinforcement steel. 2. Pull-out tests. 1983.
41. Beliaev M., Semenov A., Semenov S., Benin A. Simulation of pulling the reinforcing bar from concrete block with account of friction and concrete damage. *MATEC Web of Conferences.* 2016. Vol. 73. No. 04010.
42. Benin A.V., Semenov A.S., Semenov S.G., Melnikov B.E. Finite element modeling of fracture processes and estimation of durability of the road bridge with account of corrosion cracking. *Magazine of Civil Engineering.* 2012. No. 7(33). Pp. 32–42. (rus)

32. Работнов Ю.Н. О механизме длительного разрушения // Вопросы прочности материалов и конструкций. М.: Изд-во АН СССР, 1959. С. 5–7.
33. Kupfer H., Hilsdorf H.K., Rusch H. Behavior of concrete under biaxial stress // Journal of the American Concrete Institute. 1969. № 66. Pp. 656–666.
34. Schwer L.E., Murry Y.D. A three-invariant smooth cap model with mixed hardening // Int. J. for Num. Anal. Mech. In Geomech. 1994. № 18. Pp. 657–688.
35. Voyiadjis G.Z., Taqieddin Z.N., Kattan P.I. Anisotropic damage–plasticity model for concrete // Int. Journal of Plasticity. 2008. № 10(24). Pp. 1946–1965.
36. Семенов А.С. Симметризация тензора эффективных напряжений для сред с анизотропной поврежденностью // Научно-технические ведомости СПБГПУ. Физико-математические науки. 2017. Т. 10. № 2.
37. Abu Al-Rub R.K., Kim S.-M. Computational applications of a coupled plasticity-damage constitutive model for simulating plain concrete fracture // Engineering Fracture Mechanics. 2010. № 10(77). Pp. 1577–1603.
38. Беляев М.О., Семёнов А.С. Локализация деформаций при четырехточечном изгибе армированной бетонной балки // Материалы Научного форума с международным участием. Неделя науки СПбПУ. 2015. С. 60–62.
39. Häussler-Combe U., Hartig J. Formulation and numerical implementation of a constitutive law for concrete with strain-based damage and plasticity // International Journal of Non-Linear Mechanics. 2008. № 43. Pp. 399–415.
40. RILEM/CEB/FIB. Recommendation on reinforcement steel for reinforced concrete. RC6. Bond test for reinforcement steel. 2. Pull-out tests. 1983.
41. Beliaev M., Semenov A., Semenov S., Benin A. Simulation of pulling the reinforcing bar from concrete block with account of friction and concrete damage // MATEC Web of Conferences. 2016. № 73. № 04010.
42. Бенин А.В., Семёнов А.С., Семёнов С.Г., Мельников Б.Е. Конечно-элементное моделирование процессов разрушения и оценка ресурса элементов автодорожного моста с учётом коррозионных повреждений // Инженерно-строительный журнал. 2012. № 7(33). С. 32–42.

Andrey Benin,
+7(921)911-50-80; benin.andrey@mail.ru

Artem Semenov,
+7(905)272-11-88;
Semenov.Artem@googlemail.com

Sergey Semenov,
+7(921)983-44-56; ssgrus@gmail.com

Mikhail Beliaev,
+7(911)733-87-09; belyaev-m-o@yandex.ru

Victor Modestov,
+7(904)335-22-22; modestov@compmechlab.com

Андрей Владимирович Бенин,
+7(921)911-50-80;
эл. почта: benin.andrey@mail.ru

Артем Семенович Семенов,
+7(905)272-11-88;
эл. почта: Semenov.Artem@googlemail.com

Сергей Георгиевич Семенов,
+7(921)983-44-56; эл. почта: ssgrus@gmail.com

Михаил Олегович Беляев,
+7(911)733-87-09;
эл. почта: belyaev-m-o@yandex.ru

Виктор Сергеевич Модестов,
+7(904)335-22-22;
эл. почта: modestov@compmechlab.com

Бенин А.В., Семенов А.С., Семенов С.Г., Беляев М.О., Модестов В.С. Методы идентификации упруго-пластических моделей бетона с учетом накопления повреждений // Инженерно-строительный журнал. 2017. № 8(76). С. 279–297.